Composite nature of exotic states from data analysis

康现伟

xwkang@bnu.edu.cn

北京师范大学

高能所理论室，2022年6月29日

PRD2016，EPJC2017，PRD2022，EPJC2022

Outline

- Two concepts: CDD pole and compositeness
- X(3872)
- Z_b states
- $f_0(980)$ and $a_0(980)$

Introduction

- A series of exotic hadron candidate XYZ were and are observed, cannot be accommodated by potential model — kinematical effects, molecular, quark-gluon hybrid, et al..
- Typically different scenarios predicts different constituents, in practice, may involve several mechanism
  $\longrightarrow$ compositeness
- Stay close to threshold of meson pairs: only 2-3 MeV above meson pair threshold
  $\longrightarrow$ effective range expansion (ERE)

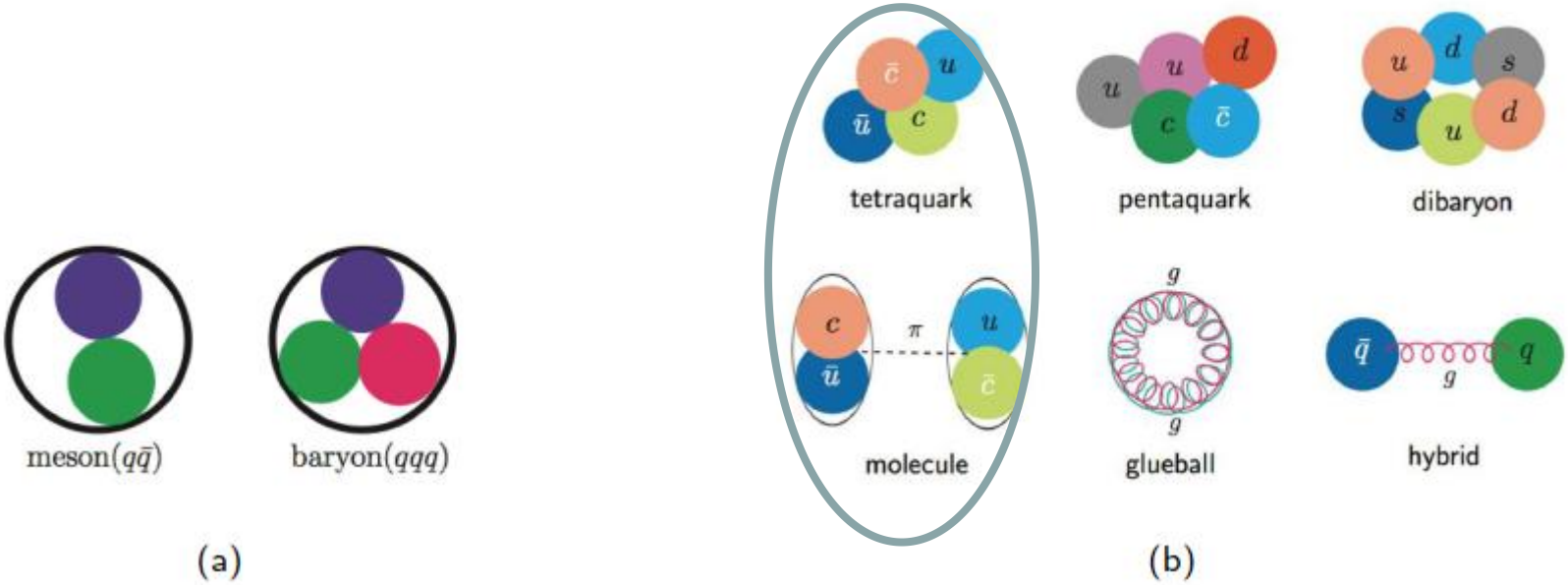

Compositeness X: weight of two-meson components in the configuration of configuration

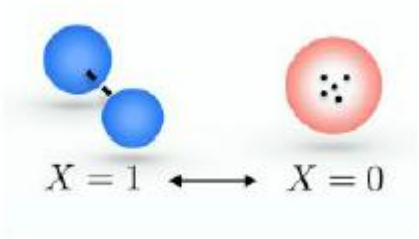

Compositeness for resonance

- Weinberg compositeness condition: wave function renormalization constant Z=0. In fact, $Z = 1 - X$, where $X = -\gamma^2 \frac{dG(s_R)}{ds_R}$ quantifies the weight of constituents; γ is the residue for $t(s)$ in the 1st sheet at the pole, and G is the two-point loop function.
- only applied to bound state — model-independent relation for deuteron [Weinberg 1963; 1965]
- For resonance case, as long as $\sqrt{\mathrm{Re}E_R^2}$ larger than the lightest threshold, $X = |\gamma^2 \frac{dG(s_R)}{s_R}|$, γ residue in the 2nd sheet [Guo and Oller, PRD2015]
- Adapted to non-relativistic case, criterion: $M_R > M_{\mathrm{th}}$, applied to Z_b and Z_c states [Kang, Guo and Oller, PRD2016]

PHYSICAL REVIEW VOLUME 101, NUMBER 1 JANUARY 1, 1956

Low's Scattering Equation for the Charged and Neutral Scalar Theories*

L. CASTILLEJO† AND R. H. DALITZ,‡ *Laboratory of Nuclear Studies, Cornell University, Ithaca, New York*

AND

F. J. DYSON, *Institute for Advanced Study, Princeton, New Jersey*

(Received August 3, 1955)

CDD poles

The Low scattering equation is studied in the one-meson approximation with both charged and neutral scalar meson theories. The general solution is found for each of these cases. It has the general character of a Wigner-Eisenbud dispersion formula and contains an infinite number of adjustable parameters. It follows that the Low equation, in this approximation at least, does not determine the scattering, but only expresses a property of the scattering which is independent of the internal structure of the scatterer.

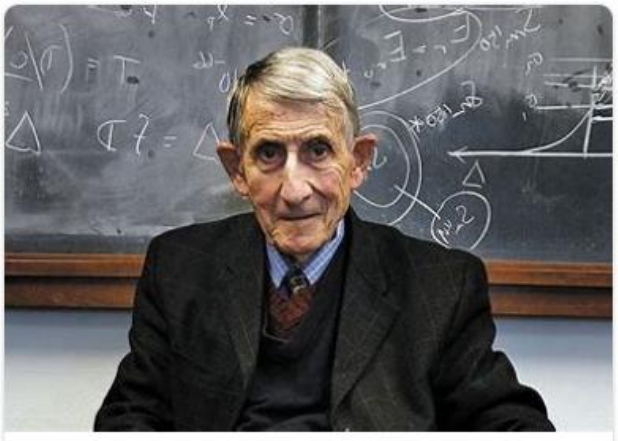

F. J. Dyson

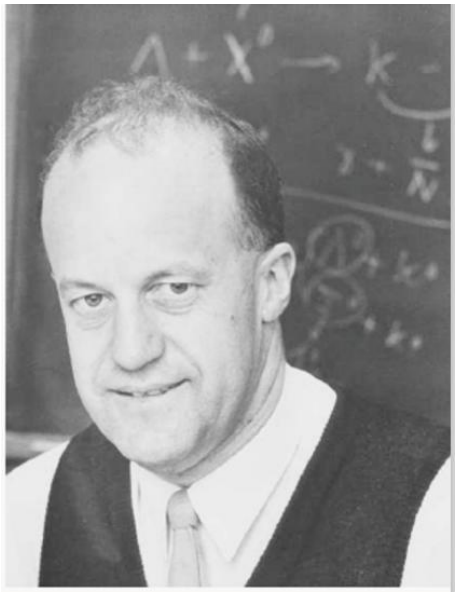

R. Dalitz

Searching for “CDD pole” on web

Dispersion relations and Castillejo-Dalitz-Dyson pole in the ...
https://pubmed.ncbi.nlm.nih.gov/9954130
Dispersion relations and Castillejo-Dalitz-Dyson pole in the pi N P wave scattering amplitude Phys Rev C Nucl Phys. 1987 Aug;36(2):714-719. doi: 10.1103/physrevc.36.714. Author K Nakano.…

UNITARIZATION, CASTILLEJO--DALITZ--DYSON POLES, ...
https://www.osti.gov/biblio/4735346
OSTI.GOV Journal Article: UNITARIZATION, CASTILLEJO--DALITZ--DYSON POLES, AND SCALAR COMPANIONS. UNITARIZATION, CASTILLEJO--DALITZ--DYSON POLES, AND…

Castillejo-Dalitz-Dyson zeros in the Pomeranchukon ...
https://www.osti.gov/biblio/4255835-castillejo-dalitz-dyson-zeros-pomeranchukon...
OSTI.GOV Journal Article: Castillejo-Dalitz-Dyson zeros in the Pomeranchukon scattering amplitude. Castillejo-Dalitz-Dyson zeros in the Pomeranchukon scattering amplitude. Full Recor…

Unitarization, Castillejo-Dalitz-Dyson Poles, and Scalar ...
https://ui.adsabs.harvard.edu/abs/1971PhRvD...4..900R/abstract
It is shown how Castillejo-Dalitz-Dyson poles may be introduced into the effective-range formulas for scalar (I=J=0) ππ and (I=J=12) Kπ form factors derived from current algebra and a method o…

两粒子弹性散射过程满足 $\mathrm{Im}T_L^{(-1)} = -\rho(s)$

$$T_L(s+i\epsilon) - T_L(s-i\epsilon) = 2i\mathrm{Im}T_L(s)$$

$$\rho(s) = \frac{k}{8\pi\sqrt{s}}$$

$$k = \frac{\sqrt{(s-(m_1+m_2)^2)(s-(m_1-m_2)^2)}}{2\sqrt{s}}$$

N/D方法简述

分波振幅$T_L(s)$: $T_L(s) = \dfrac{N_L(s)}{D_L(s)}$

$D_L(s)$：包含右手割线；$N_L(s)$：左手割线

仅考虑右手割线，从幺正关系得到：

$$\mathrm{Im}D_L = \mathrm{Im}T_L^{-1}N_L = -\rho(s)N_L, \quad s > s_{\mathrm{th}}$$

$$\mathrm{Im}D_L = 0, \quad s < s_{\mathrm{th}}$$

N/D方法简述

分波振幅$T_L(s)$: $T_L(s) = \dfrac{N_L(s)}{D_L(s)}$

$D_L(s)$：包含右手割线；$N_L(s)$：左手割线

仅考虑右手割线，从幺正关系得到：

$$\mathrm{Im}D_L = \mathrm{Im}T_L^{-1}N_L = -\rho(s)N_L, \quad s > s_{\mathrm{th}}$$

$$\mathrm{Im}D_L = 0, \quad s < s_{\mathrm{th}}$$

$$D_L(s) = -\frac{(s-s_0)^{L+1}}{\pi}\int_{s_{\mathrm{th}}}^{\infty} ds' \frac{\rho(s')}{(s'-s)(s'-s_0)^{L+1}} + \sum_{m=0}^{L} a_m s^m + \sum_{i}^{M_L} \frac{\gamma_i}{s-s_i}$$

- 其中：M_L是CDD极点的数目，该项来自函数中CDD极点的出现，求和项与CDD极点一一对应。

(1) 添加这些CDD极点不违背任何解析性、幺正性的要求

(2) CDD极点是T振幅的零点

(3) CDD极点的出现：与分波振幅有相同量子数的基本粒子相关联

- M_{CDD} close to M_{th}, then small X, i.e., containing also other important components, e.g., compact quark-gluon states; M_{CDD} far from M_{th}, then the two meson constitute dominates

Approximation for left-hand cut contribution

$$N(s) = 1,$$

$$D(s) = \sum_i \frac{\gamma_i}{s - s_i} + a - \frac{(s - s_0)}{\pi} \int_{s_{\text{th}}}^{\infty} ds' \frac{\rho(s')}{(s' - s)(s' - s_0)}.$$

$$T(s) = \frac{1}{D_L} = \left[\sum_i \frac{\gamma_i}{s - s_i} + G(s) \right]^{-1}$$

$$G(s) = a(s_0) + \frac{s - s_0}{\pi} \int_{s_i}^{\infty} ds' \frac{\rho(s')}{(s' - s)(s' - s_0)}$$

函数$G(s)$

积分部分：一次减除色散关系

- 两介子圈函数

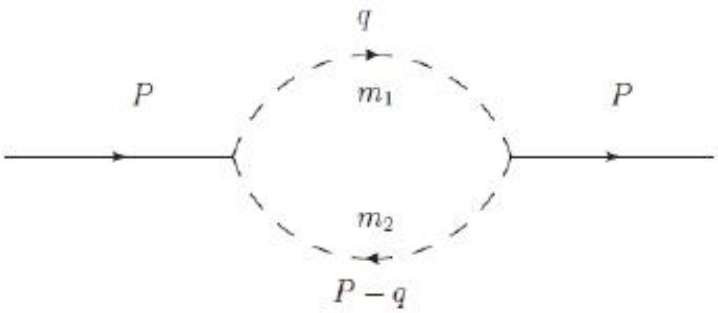

$$G(s)=\alpha(\mu^2)+\frac{1}{(4\pi)^2}\left(\log\frac{m_2^2}{\mu^2}-\varkappa_+\log\frac{\varkappa_+-1}{\varkappa_+}-\varkappa_-\log\frac{\varkappa_--1}{\varkappa_-}\right)$$

$$\varkappa_\pm=\frac{s+m_1^2-m_2^2}{2s}\pm\frac{k}{\sqrt{s}},$$

$$k=\frac{\sqrt{(s-(m_1-m_2)^2)(s-(m_1+m_2)^2)}}{2\sqrt{s}}$$

Inclusion of CDD pole and ERE

- Only right-hand cut without crossed-channel effect [Oller and Oset, PRD1999] $t(E) = \left[\sum_i \frac{g_i}{E - M_{\mathrm{CDD},i}} + \beta - ik\right]^{-1}$
- ERE: $t(E) = \left[-1/a + 1/2\, r\, k^2 - ik\right]^{-1}$
- Expansion of Re $t(E)^{-1}$ in powers of k^2 is equivalent to ERE, but worry for the small scale $[M_{\mathrm{CDD}} - M_{\mathrm{th}}]$, which restricts the validity range.
- M_{CDD} far away from M_{th}, then modulu of r is around 1 fm, otherwise r is very large.

$$1/a = \frac{g_i}{M_{\mathrm{CDD}} - M_{\mathrm{th}}} - \beta, \quad r = -\frac{g_i}{\mu (M_{\mathrm{th}} - M_{\mathrm{CDD}})^2}$$

Classification of poles in S matrix

from Tetsuo Hyodo

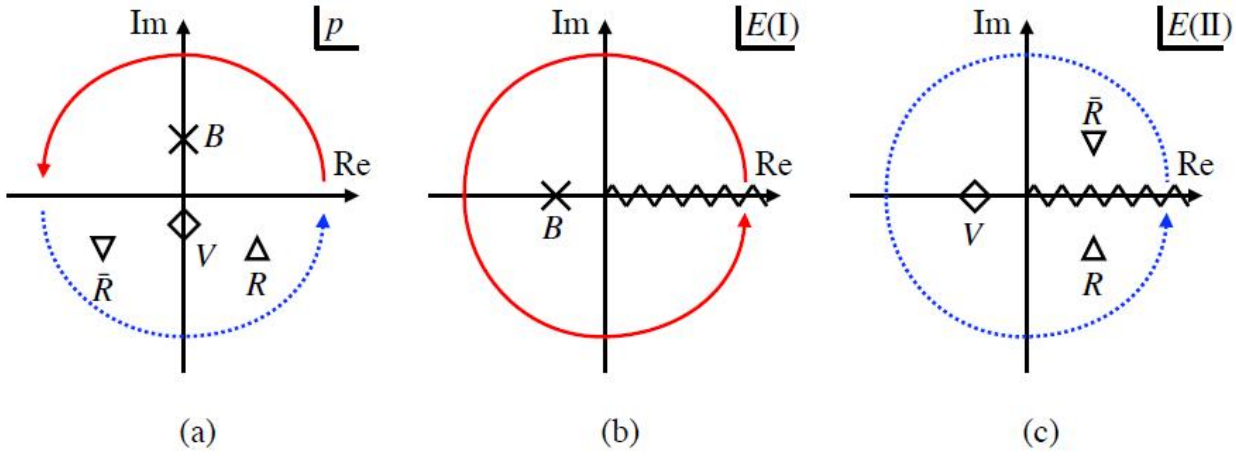

Figure 10: Poles in complex plane. (a) : p plane, (b) : E plane (1st Riemann sheet), (c) : E plane (2nd Riemann sheet). B, V, R, and $\bar{R}$ represent bound state, virtual state, resonance, and Anti-resonance.

- X(3872) state

- First observation from Belle, PRL2003, triggering voluminous amount of papers
- PDG determination:

$$I^G(J^{PC}) = 0^+(1^{++}),$$
$$M = 3871.69 \pm 0.17 \text{ MeV}, \Gamma < 1.2 \text{ MeV}, \text{ CL} = 90\%$$
$$\bar{D}D^* : C = + \text{ combination } (D\bar{D}^* + \bar{D}D^*)/\sqrt{2}$$
$$\text{threshold } M_{\text{th}} = 3871.81 \text{ MeV}$$

- From now on, all the energy and M_{CDD} are measured respective to M_{th}. X(3872) mass: -0.11 ± 0.17 MeV
- Nature: molecular like virtual state (V) and bound state (B), or preexisting state, etc.

Nature of $X(3872)$

- V or B scenarios are typically based on ERE analysis
  [Hanhart et al PRD76,034007('07); Braaten et al PRD81, 014019('10)]
- But as mentioned, a nearby CDD pole around threshold could spoil ERE strongly. Recall previous slide!
- all these scenarios can not be excluded
- New points: these are obtained by parameterizing data in more general terms
  - a simultaneous virtual and bound state (V+B);
  - double/triple virtual state $\rightarrow$ higher-order S-matrix pole.

Experimental situation: $\bar{D}^0 D^{*0}$ channel

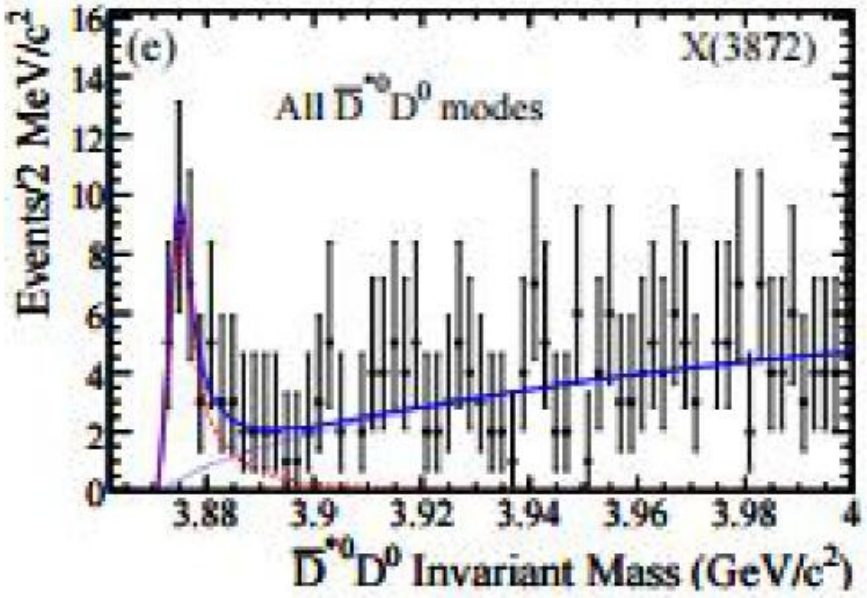

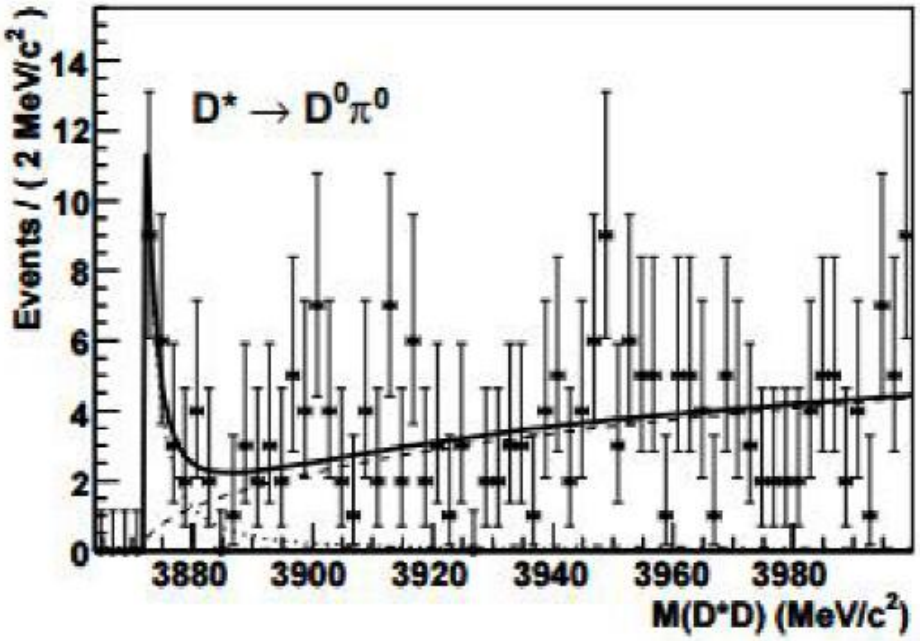

- the decay chain: $B \to X(3872)K \to \bar{D}^0 D^{*0} K$
- Left: BaBar2008, Right: Belle2010
- BaBar has total number of $B\bar{B}$ pairs, $N_{B\bar{B}}^{\mathrm{BaBar}} = 3.83 \cdot 10^8$, while $N_{B\bar{B}}^{\mathrm{Belle}} / N_{B\bar{B}}^{\mathrm{BaBar}}$=1.75

Experimental situation: $J/\psi\pi\pi$ channel

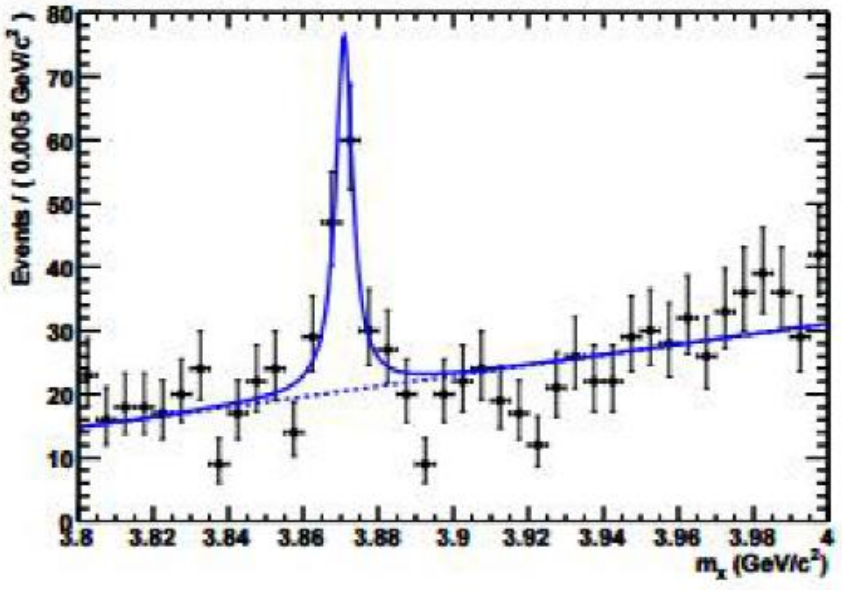

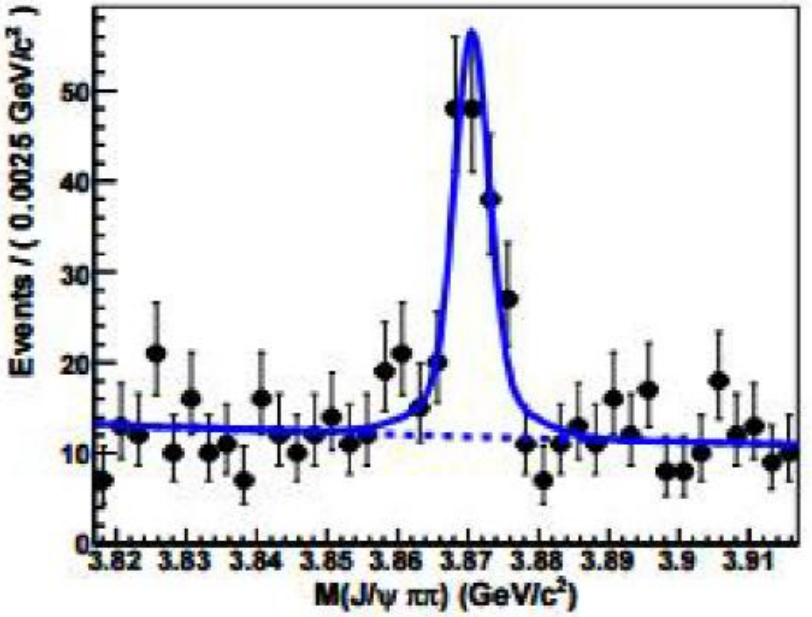

- the decay chain: $B \to X(3872)K \to J/\psi\pi^+\pi^-K$
- Left: BaBar2008, Right: Belle2008
- Data are compatible with each other.

Experimental situation: $J/\psi\pi\pi$ channel continued

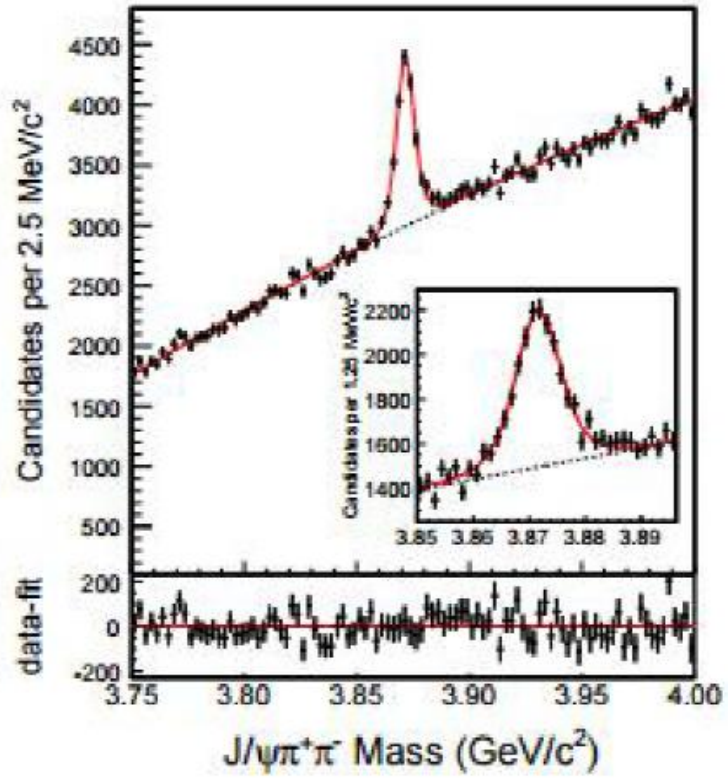

- the decay chain: $p\bar{p} \to X(3872) +$ all with $X(3872) \to J/\psi\pi^+\pi^-$
- The inset shows an enlargement of the region around the $X(3872)$ peak, with very small bin width of 1.25 MeV.
- *"Precision Measurement of the $X(3872)$ in $J/\psi\pi\pi$ Decays"* from CDF2009.

Formalism (1)

- Exp summary: Belle $D\bar{D}\pi$ + BaBar $J/\psi\pi\pi$ + Belle $J/\psi\pi\pi$ + CDF $J/\psi\pi\pi$
- As introduced, scattering amplitude

$$t(E) = \left(\frac{\lambda}{E - M_{\text{CDD}}} + \beta - ik(E) \right)^{-1},$$

more general than ERE

- Removing the extra zeros due to the CDD pole, one ends with the final-state interaction

$$d(E) = \left(1 + \frac{E - M_{\text{CDD}}}{\lambda} (\beta - ik) \right)^{-1}$$

[Oller PLB2000, Bugg PLB2003]

- When M_{CDD} far, $M_{\text{CDD}} \to \infty$ keeping λ / M_{CDD} fixed, one recovers the scattering length approximation

$$t(E) \Longrightarrow f(E) = \frac{1}{-\lambda / M_{\text{CDD}} + \beta - ik} = \frac{1}{-\gamma - ik}$$

Formalism (2)

- The normalized standard non-relativistic mass distribution for a narrow resonance or bound state ($\Gamma_X \to 0$)

$$\frac{d\hat{M}}{dE} = \frac{\Gamma_X |d(E)|^2}{2\pi|\alpha|^2}$$

- α is a constant, obtained by singling out the pole contribution, in fact, the residue of $d(E)$, $d(E) \sim \frac{\alpha}{E-E_p}$, E_p pole position.
- Normalization integral $\mathcal{N} = \int_{-\infty}^{\infty} dE \frac{d\hat{M}}{dE}$
- For a narrow resonance (including bound state), $\mathcal{N} \approx 1$, but not so when $d(E)$ has a shape strongly departs from a non-relativistic Breit-Wigner, e.g., for a virtual state
- For $f(E)$ (ERE), the integral does not converge, just integrate in the signal region.

Formalism (3): event distribution for $J/\psi\pi\pi$ channel

- For $B \to KJ/\psi\pi\pi$ channel [simpler]:

$$N_i = 2N_{B\bar{B}}\left[\mathcal{B}_J \int_{E_i-\Delta/2}^{E_i+\Delta/2} dE' \int_{-\infty}^{\infty} dE R(E', E)\frac{d\hat{M}}{dE} + \text{cbg}_J\Delta\right]$$

- For $p\bar{p}$ to $J/\psi\pi\pi$ channel: just replace $2N_{B\bar{B}}$ by $\mathcal{L}\sigma_{p\bar{p}\to X\text{All}}$, with $\mathcal{L}$ luminosity, and total cross section σ for $p\bar{p} \to X + \text{All}$.
- $R(E', E)$ is the Gaussian, experimental resolution function
- $\int_{E_i-\Delta/2}^{E_i+\Delta/2} dE'$ indicates the integration in the bin width.

Formalism (4): event distribution for $\bar{D}^0 D^{*0}$ channel

- For $B \to K \bar{D}^0 D^{*0}$ channel [taking into account the small width of D^*, $\Gamma_* \approx 65$ KeV]

$$N_i = 2N_{B\bar{B}} \int_{E_i-\Delta/2}^{E_i+\Delta/2} dE' \int_0^\infty d\mathcal{E}' R(E', \mathcal{E}') \sqrt{\mathcal{E}'} \times \left[\frac{\mathcal{B}_D \Gamma_*}{\sqrt{2}\pi \left(\sqrt{E_X^2 + \Gamma_*^2/4} - E_X \right)^{1/2}} \int_{-\infty}^{\infty} dE \frac{d\hat{M}}{dE} \frac{1}{|\mathcal{E}' - E - i\Gamma_*/2|^2} + \text{cbg}_D \right]$$

- Pole position $E_X - i\Gamma_X/2$, with E_X relative to $\bar{D}^0 D^{*0}$ (reduced mass $\mu \approx 1$GeV) threshold, momentum at pole position k_X.

Fit strategy

- $\mathcal{B}_D$, $\mathcal{B}_J$, cbg_D, cbg_J, overall constants and background are always free parameters
- As mentioned, for bound state, $\mathcal{B}$ can be justified as branching ratio, otherwise not.
- M_{CDD}, λ, β characterize the line shape of $d(E)$.
- Braaten et al has also used ERE (only scattering length), but fit separately
- C. Hanhart et al used ERE including the effective range.
- One should use more general $d(E)$, other than ERE!
- Maximize likelihood fit, data errors are asymmetric.

Different scenarios

- Case i): using ERE, which is a pure bound state, making combined fits to all the existing data
- Case ii): imposing $t(E)$ has a virtual state, one can express λ and β from E_R and M_{CDD}.
- Case iii): taking into account the coupled channel effect, E_R determines the shape of $t(E)$:
  Quadratic equation: two solutions with case iii). I and case iii).II

Results

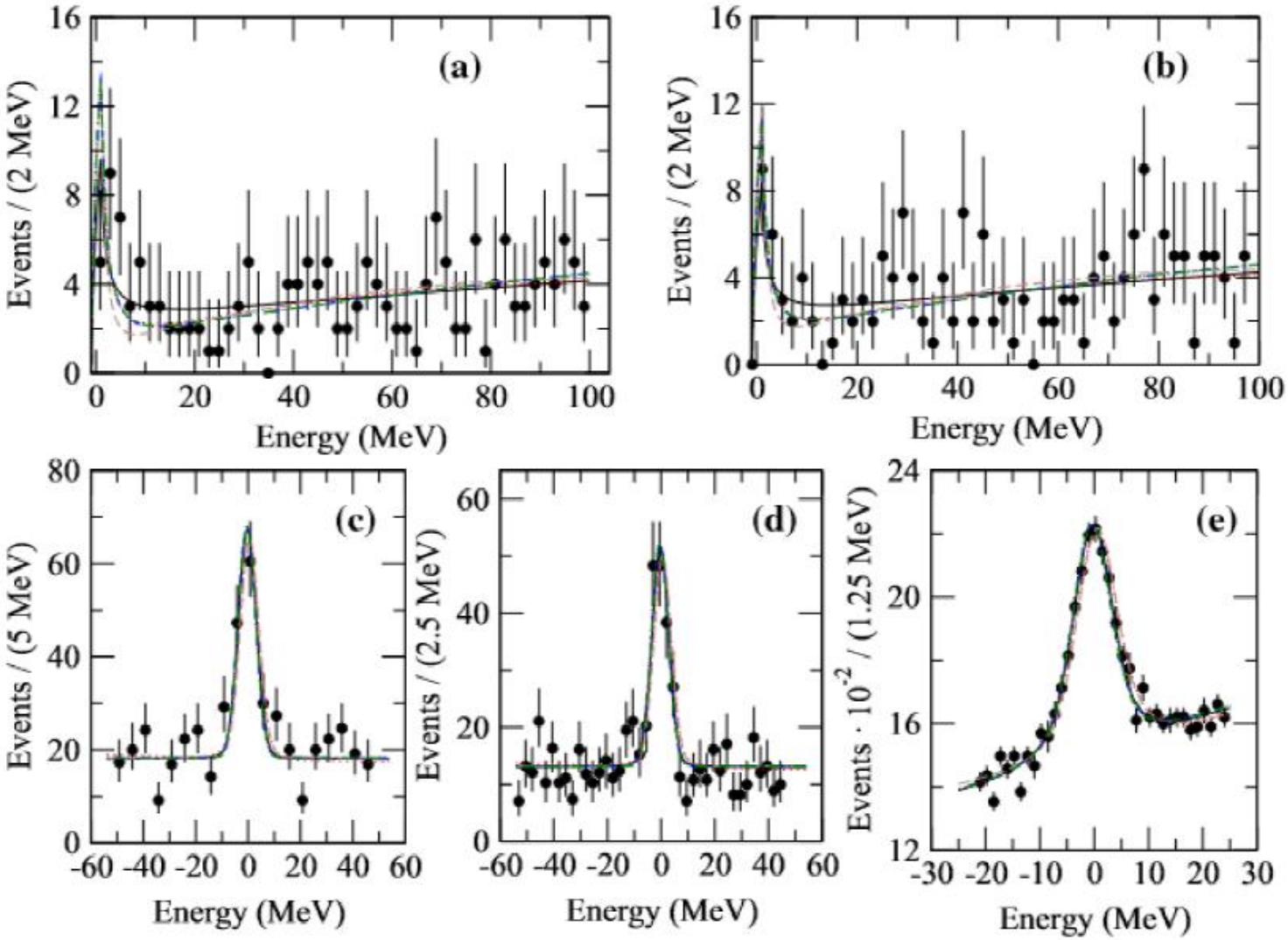
(a)
Events / (2 MeV)
Energy (MeV)
(b)
Events / (2 MeV)
Energy (MeV)
(c)
Events / (5 MeV)
Energy (MeV)
(d)
Events / (2.5 MeV)
Energy (MeV)
(e)
Events · 10^-2 / (1.25 MeV)
Energy (MeV)

Results

Cases	Pole position [MeV]	X	Residue [GeV^2]	Y_{D1} Y_{D2} Y_J $Y_J^{(p)}$
1	$-0.19^{+0.01}_{-0.01} - i\,0.0325$	1.0	$14.78^{+0.38}_{-0.14}$	$7.49^{+0.71}_{-0.41}$ $6.45^{+0.32}_{-0.47}$ $79.03^{+5.65}_{-6.11}$ $5.23^{+0.07}_{-0.11} \times 10^3$
2.I	$-0.36^{+0.08}_{-0.10} - i\,0.18^{+0.01}_{-0.02}$ $-0.70^{+0.11}_{-0.13} + i\,0.17^{+0.02}_{-0.01}$		$-47.48^{+9.75}_{-12.40} - i\,66.06^{+10.87}_{-13.50}$ $82.69^{+14.84}_{-11.88} + i\,66.03^{+13.50}_{-10.87}$	$83.13^{+22.42}_{-16.15}$ $40.13^{+11.86}_{-7.25}$ $8.44^{+3.64}_{-2.59} \times 10^3$ $5.78^{+2.29}_{-1.65} \times 10^5$
2.II	$-0.33^{+0.04}_{-0.03} - i\,0.31^{+0.02}_{-0.01}$ $-0.84^{+0.07}_{-0.05} + i\,0.77^{+0.03}_{-0.04}$ $-1.67^{+0.10}_{-0.08} - i\,0.49^{+0.02}_{-0.02}$		$-6.24^{+2.80}_{-2.20} - i\,1.41^{+0.14}_{-0.10} \times 10^2$ $(2.32^{+0.16}_{-0.21} - i\,1.77^{+0.11}_{-0.08}) \times 10^2$ $(-3.26^{+0.22}_{-0.16} + i\,3.18^{+0.18}_{-0.25}) \times 10^2$	$79.75^{+22.46}_{-19.81}$ $42.20^{+9.18}_{-8.02}$ $9.23^{+1.60}_{-1.57} \times 10^3$ $6.23^{+0.71}_{-0.84} \times 10^5$
3.I	$-0.50^{+0.04}_{-0.03}$ $-0.68^{+0.05}_{-0.03}$	$0.061^{+0.003}_{-0.002}$	$1.52^{+0.01}_{-0.01}$ $2.72^{+0.02}_{-0.04}$	$25.45^{+4.05}_{-4.15}$ $12.29^{+1.32}_{-1.89}$ $80.14^{+5.67}_{-5.19}$ $5.26^{+0.12}_{-0.08} \times 10^3$
3.II	$-0.51^{+0.03}_{-0.01}$ $-1.06^{+0.05}_{-0.02}$	$0.158^{+0.001}_{-0.001}$	$3.96^{+0.03}_{-0.08}$ $7.56^{+0.08}_{-0.20}$	$22.90^{+2.94}_{-3.02}$ $11.03^{+1.40}_{-0.77}$ $80.07^{+5.14}_{-5.36}$ $5.28^{+0.05}_{-0.17} \times 10^3$

- Z_b states

Belle合作组

PRL 116.212001(2016)

Three-body analysis of

$$e^+e^- \to B\bar{B}\pi^\pm, B\bar{B}^*\pi^\pm, B^*\bar{B}^*\pi^\pm$$

First observation of
$Z_b(10610)$ and $Z_b(10650)$

$M_{Z_b} = 10607.2 \pm 2.0$ MeV, $\Gamma_{Z_b} = 18.4 \pm 2.4$ MeV;

$M_{Z_b'} = 10652.2 \pm 1.5$ MeV, $\Gamma_{Z_b'} = 11.5 \pm 2.2$ MeV.

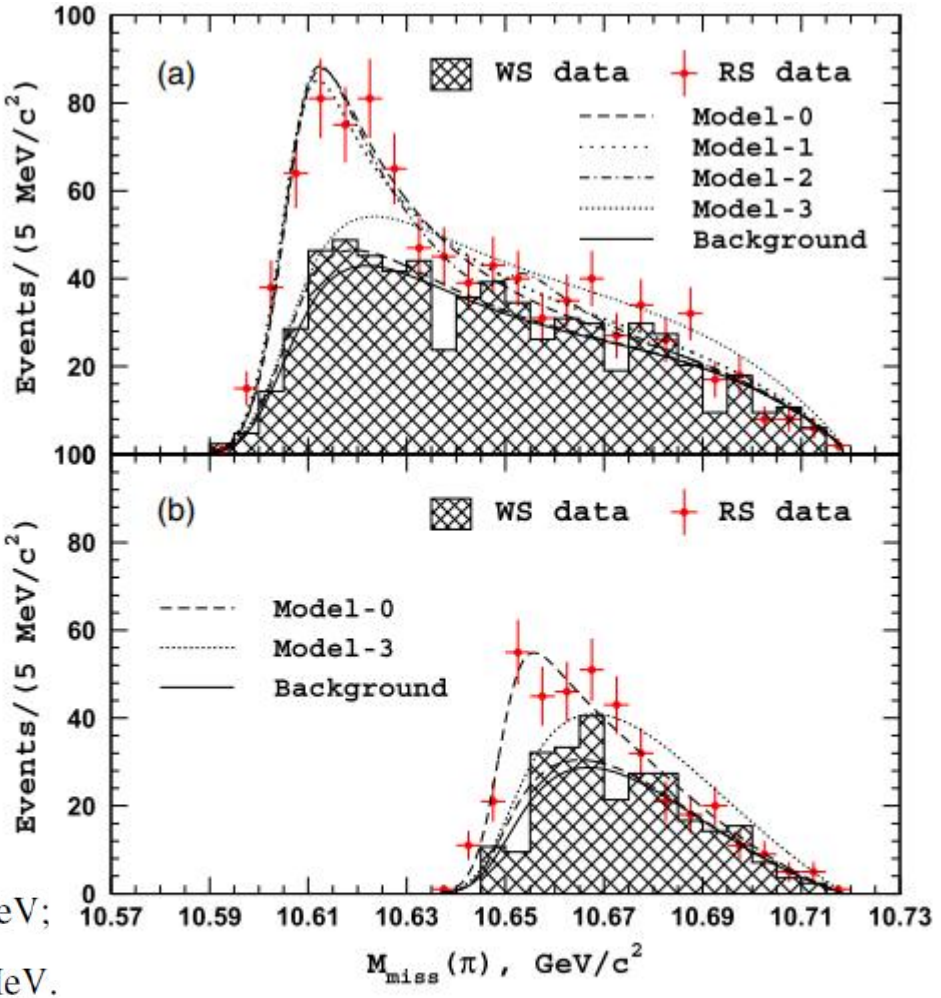

FIG. 2. The $M_{\rm miss}(\pi)$ distribution for the (a) $BB^*\pi$ and (b) $B^*B^*\pi$ candidate events. Normalization factor is applied for the WS distributions.

不同理论方法：介子分子态理论，cusp效应，紧凑四夸克态，
夸克-胶子混合态，以及强子夸克偶素态

模型区别：对共振态内部组成的不同假设

What can we learn from the data about its inner structure including the compositeness coefficient?

a single channel analysis is qualified, at least as a first approximation

TABLE III. B branching fractions for the $Z_b^+(10610)$ and $Z_b^+(10650)$ decays. The first quoted uncertainty is statistical, the second is systematic.

Channel	Fraction, %	
	$Z_b(10610)$	$Z_b(10650)$
$\Upsilon(1S)\pi^+$	$0.54^{+0.16+0.11}_{-0.13-0.08}$	$0.17^{+0.07+0.03}_{-0.06-0.02}$
$\Upsilon(2S)\pi^+$	$3.62^{+0.76+0.79}_{-0.59-0.53}$	$1.39^{+0.48+0.34}_{-0.38-0.23}$
$\Upsilon(3S)\pi^+$	$2.15^{+0.55+0.60}_{-0.42-0.43}$	$1.63^{+0.53+0.39}_{-0.42-0.28}$
$h_b(1P)\pi^+$	$3.45^{+0.87+0.86}_{-0.71-0.63}$	$8.41^{+2.43+1.49}_{-2.12-1.06}$
$h_b(2P)\pi^+$	$4.67^{+1.24+1.18}_{-1.09-0.89}$	$14.7^{+3.2+2.8}_{-2.8-2.3}$
$B^+\bar{B}^{*0} + \bar{B}^0 B^{*+}$	$85.6^{+1.5+1.5}_{-2.0-2.1}$	...
$B^{*+}\bar{B}^{*0}$	...	$73.7^{+3.4+2.7}_{-4.4-3.5}$

Coupled-channel effect is indeed small, on theory side

- Effective range expansion (ERE) could be a proper tool to study the physics in the vicinity of threshold. elastic isovector S-wave $\bar{B}B^*$ scattering. No specific dynamics is assumed.
- However, at pole position, momentum (modulus of complex values) is around m_π (pion mass). Left-hand branch point happens from $im_\pi/2$, inside the circle of the convergence radius, which prevents the validity of ERE.
- However, the pion exchange are suppressed. Specific calculation exists [Valderrama PRD2012; Hong-Wei Ke et al. JHEP2012, Dias PRD2015; Dian-Yong Chen and Xiang Liu, PRD2011]
- Chiral EFT power counting also shows coupled-channel effects are also suppressed. [Valderrama PRD2012]

OZI suppression

- The light meson ($q\bar{q}$) exchange violates OZI rule for $I = 1$ sector. Two-meson exchange contributes as the lowest-order.
- $B\bar{B}\pi$ vertex does not exists, but $B\bar{B}\rho$ and $B\bar{B}\omega$ do. Total contribution vanishes if ρ and ω are taken as equal mass. [Dias et al., PRD2015]

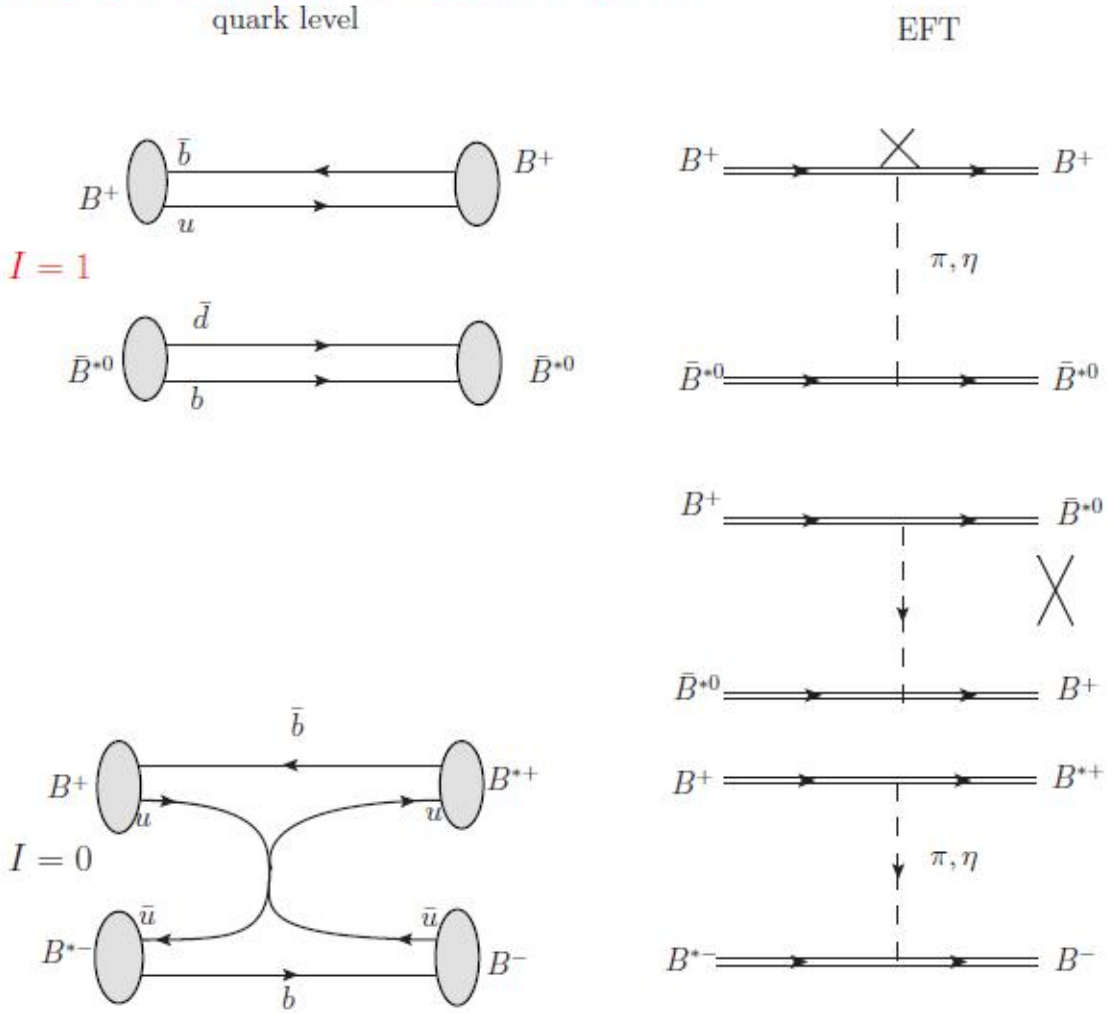

非相对论情况

$$t(E) = 8\pi m_{\rm th}\left[\frac{\lambda}{E - M_{\rm CDD}} + \beta - ik\right]^{-1}$$

其中

$$\lambda = \gamma^2 \frac{8\pi m_{\rm th}}{m_{\rm th} + M_{\rm CDD}},$$

$$\beta = 8\pi m_{\rm th}\alpha(\mu^2) + \frac{1}{\pi}\left(m_1 \log\frac{m_1}{\bar{\mu}} + m_2 \log\frac{m_2}{\bar{\mu}}\right)$$

$$k = \sqrt{2\bar{\mu}(E - m_{\rm th})}.$$

非相对论极限下，满足幺正性条件：

$$Imt^{-1}(E) = -k/8\pi m_{th}$$

第二黎曼面分波振幅

$$t^{II}(E) = 8\pi m_{\rm th}\left[\frac{\lambda}{E - M_{\rm CDD}} + \beta + ik\right]^{-1}$$

$Im\ k > 0$ 成立

能量依赖的事例数分布

影响因素

背景参数化：$B(E) = b_0 e^{-\alpha(E-(m_B+m_{B^*}))}\epsilon(E)F_{\mathrm{PHSP}}(E)$,

效率表达式：$\epsilon(E) \sim \exp[(E - m_0)/\Delta_0](1 - E/m_0)^{3/4}$

效率阈值为$m_0 = 10.718 \pm 0.001\mathrm{GeV}/c^2$

系数$\Delta_0 = 0.094 \pm 0.002\mathrm{GeV}/c^2$

相空间函数：$F_{\mathrm{PHSP}}(E) \sim |\vec{P}_B||\vec{P}_\pi|$,

$$|\vec{P}_B| = \frac{1}{2E}\left[\left(E^2 - (m_B + m_{B^*})^2\right)\left(E^2 - (m_B - m_{B^*})^2\right)\right]^{1/2},$$

$$|\vec{P}_\pi| = \frac{1}{2M_{\Upsilon(10860)}}\left[\left(M^2_{\Upsilon(10860)} - (E + m_\pi)^2\right)\left(M^2_{\Upsilon(10860)} - (E - m_\pi)^2\right)\right]^{1/2}$$

分辨率函数：$R(E', E) = \frac{1}{\sqrt{2\pi}\sigma}\exp\left(-\frac{(E' - E)^2}{2\sigma^2}\right)$

$\sigma = 6.0\ \mathrm{MeV}/c^2$

事例数分布：$B^{(*)}\bar{B}^*$ 不变质量的函数

$$N(E) = N_{\Upsilon(10860)}\epsilon(E)\int_{m_{\mathrm{th}}}^{M_{\Upsilon(10860)}-m_\pi}[Y_{Z_b}|d(E')|^2 + B(E')]F_{\mathrm{PHSP}}(E')R(E', E)dE'$$

$$d(E) = \frac{1}{1 + \frac{E - M_{\mathrm{CDD}}}{\lambda}(\beta - ik)}$$

⇐ **Signal $|d(E)|^2$**

- E：$B^{(*)}\bar{B}^*$体系的不变质量
- Belle探测器中亮度：$121.4fb^{-1}$
- $\Upsilon(10860)$总的事例数观测数值：$N_{\Upsilon(10860)} \approx 1.24 \times 10^8$

拟合方案

	背景项	归一化常数	d(E)
参数	b_0, α	Y_Z	λ, M_{CDD}, β

共振态E_P是$t^{II}(E)$函数的极点：

$$\boldsymbol{t^{II}(E)^{-1}=0}$$

$$\lambda = \frac{1}{2\Gamma_{Z_b}}(\Gamma_{Z_b}^2 + 4\Delta^2)v\cos u, \quad \beta = \frac{v}{\Gamma_{Z_b}}(-2\Delta\cos u + \Gamma_{Z_b}\sin u),$$

$$u \equiv \frac{1}{2}\arg\left(M_{Z_b} - m_{\mathrm{th}} + i\frac{\Gamma_{Z_b}}{2}\right), \quad v \equiv \left(\mu\sqrt{4(M_{Z_b} - m_{\mathrm{th}})^2 + \Gamma_{Z_b}^2}\right)^{1/2}, \quad \Delta \equiv M_{Z_b} - M_{\mathrm{CDD}}$$

- 需拟合参数：b_0, α, Y_{Z_b}, M_{CDD}
- M_{CDD}：由描述信号形状的$d(E)$函数确定，与组分系数X相关

数值结果

◆ 共振态不变质量分布的拟合结果

	b_0	α [GeV^{-1}]	Y_{Z_b} [10^{-3}GeV^{-1}]	$M_{\mathrm{CDD}} - m_{\mathrm{th}}$ [MeV]	χ^2/dof
$Z_b(10610)$	4.87×10^{-4}	10.09	3.27	0.00	0.78
	6.32×10^{-4}	13.58	0.34	12.57	1.13
$Z_b(10650)$	1.01×10^{-3}	33.05	1.86	0.00	0.86
	1.11×10^{-3}	35.01	0.24	9.72	0.83

固定M_{CDD}为特殊值： $M_{CDD} = m_{th}$； 使得$X = 1$成立的值

调节归一化常数Y_{Z_b}的值，都可很好的拟合实验数据

数值结果

◆ 共振态不变质量分布的拟合图像

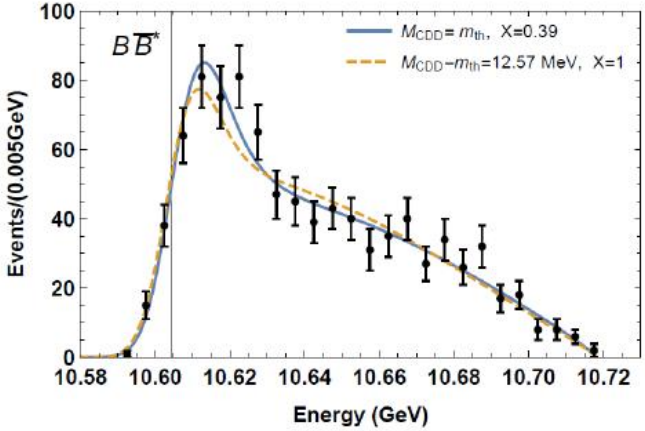

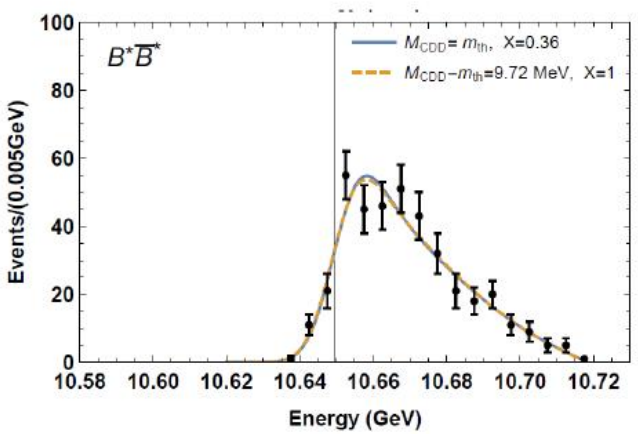

$M_{CDD}=m_{th}$：组分系数的值最小

$B\bar{B}^*$ 结构在$Z_b(10610)$共振态中，比例系数X=0.39；

$B^*\bar{B}^*$ 结构在$Z_b(10650)$共振态中，比例系数X=0.36；

X=1：对实验数据的描述十分近似

◆ 两个Z_b共振态组分系数的变化范围0.4~1.0

C. Y. Cui, Y. L. Liu and M. Q. Huang, PRD 85, 074014 (2012):
both a $B^*\overline{B}$ molecular state and a $[bd][\overline{b}\overline{u}]$ tetraquark state coincide with $Z_b(10610)$.

◆ 相关物理量的计算数值

	λ [MeV^2]	β [MeV]	γ_s^2 [GeV^2]	X	a [fm]	r [fm]
$Z_b(10610)$	1.87×10^3	73.26	$-133.06-i122.49$	0.39	–	–
	3.51×10^3	323.73	$-235.10+i404.65$	1.00	−4.44	−1.65
$Z_b(10650)$	1.11×10^3	21.65	$-80.69 - i110.91$	0.36	–	–
	2.20×10^3	286.14	$-69.37 + i380.10$	1.00	−3.31	−1.72

$M_{\mathrm{CDD}} = M_{\mathrm{th}}$，$r \to \infty$，有效力程展开失效

1. Precision of data is a crucial input
2. Probing other observables e.g., decay property, beyond the mass spectrum alone is necessary

- $f_0(980)$ and $a_0(980)$

Formulation of the compositeness relation and decay width

- We define the four Riemann Sheets according to the imaginary parts of p_1 and p_2,

$$\begin{aligned}
\text{Sheet I}: &\quad \text{Im}p_1 > 0,\ \text{Im}p_2 > 0 \\
\text{Sheet II}: &\quad \text{Im}p_1 < 0,\ \text{Im}p_2 > 0 \\
\text{Sheet III}: &\quad \text{Im}p_1 < 0,\ \text{Im}p_2 < 0 \\
\text{Sheet IV}: &\quad \text{Im}p_1 > 0,\ \text{Im}p_2 < 0
\end{aligned}$$

  p_i is the momentum of the channel i,

$$p_i(s) = \frac{\sqrt{[s-(m_1+m_2)^2][s-(m_1-m_2)^2]}}{2\sqrt{s}}$$

- We are more concerned with those non-physical Riemann Sheets which are connected to the physical one.
- Riemann Sheet II and III are connected to the physical Riemann Sheet I below and above the $K\overline{K}$ threshold in the real axis, respectively.

- Analytic continuation of $G_i(s)$

$$G_i^{II}(s+i\epsilon) = G_i^{I}(s-i\epsilon) = G_i^{I}(s+i\epsilon) - 2i\mathrm{Im}G_i^{I}(s+i\epsilon)$$
$$= G_i^{I}(s+i\epsilon) + \frac{i}{8\pi}\sqrt{\frac{[s+i\epsilon-(m_1+m_2)^2][s+i\epsilon-(m_1-m_2)^2]}{(s+i\epsilon)^2}},$$

- The corresponding $G_i(s)$ in different Riemann Sheets

$$\begin{aligned}
\text{Sheet I}: &\quad G_1^{I}(s), G_2^{I}(s),\\
\text{Sheet II}: &\quad G_1^{II}(s), G_2^{I}(s),\\
\text{Sheet III}: &\quad G_1^{II}(s), G_2^{II}(s),\\
\text{Sheet IV}: &\quad G_1^{I}(s), G_2^{II}(s),
\end{aligned}$$

Two main equations

- Assumption: saturation by two channels

$$X = X_1 + X_2 = |\gamma_1|^2 \left| \frac{\partial G_1(s)}{\partial s} \right|_{s=s_P} + |\gamma_2|^2 \left| \frac{\partial G_2(s)}{\partial s} \right|_{s=s_P}$$

- The relation between the pole width and partial decay width:

$$\Gamma_R = |\gamma_1|^2 \frac{p_1(m_R^2)}{8\pi m_R^2} \pm |\gamma_2|^2 \frac{1}{16\pi^2} \int_{m_1+m_2}^{m_R+2\Gamma_R} dW \frac{p(W^2)}{W^2} \frac{\Gamma_R}{(m_R - W)^2 + \Gamma_R^2/4},$$

- The Lorentzian mass distribution is considered in the second channel.
- The upper integration limit is cut at $m_R + 2\Gamma_R$ in the resonance region.
- The plus and minus sign correspond to RS III and II, respectively.
  $\rightarrow$ The sign of the momentum of the kaon has opposite signs in the RSs II and III.
  $\rightarrow$ $m_R - i\Gamma_1/2 + i\Gamma_2/2 = m_R - i(\Gamma_1 - 2\Gamma_2)/2 - i\Gamma_2/2$ (RS II),
  $\rightarrow$ $m_R - i\Gamma_1/2 - i\Gamma_2/2$ (RS III).

Taking r_{exp} as input

- The r_{exp} as input in terms of the branching ratio to the first channel,

$$r_{exp} = 1 - \frac{\Gamma_2}{\Gamma_R} = \frac{\Gamma_1 - 2\Gamma_2}{\Gamma_R}, \text{ RS II}$$

where the lighter channel decay width expressed as $\Gamma_{\pi\pi(\pi\eta)} = \Gamma_1 - 2\Gamma_2$

In the RS III,

$$r_{exp} = 1 - \frac{\Gamma_2}{\Gamma_R} = \frac{\Gamma_1}{\Gamma_R}, \text{ RS III}$$

- Combine with decay width relation

$$\Gamma_R = |\gamma_1|^2 \frac{p_1(m_R^2)}{8\pi m_R^2} \pm |\gamma_2|^2 \frac{1}{16\pi^2} \int_{m_1+m_2}^{m_R+2\Gamma_R} dW \frac{p(W^2)}{W^2} \frac{\Gamma_R}{(m_R - W)^2 + \Gamma_R^2/4},$$

- Two equations pin $|\gamma_1|$ and $|\gamma_2|$ down.

- Input pole parameter of $f_0(980)$:

  From the dispersive analysis, based on the use of a set of Roy-like equations called the GKPY equations [1,2]:

$$m_R = 996 \pm 7 \text{ MeV}, \quad \Gamma_R = 50^{+20}_{-12} \text{ MeV}$$

  Study of S and P-wave meson-meson scattering by unitarizing one-loop amplitude in Chira Perturbation Theory (ChPT) [3]:

$$m_R = 978^{+7}_{-11} \text{ MeV}, \quad \Gamma_R = 58^{+18}_{-22} \text{ MeV}$$

- The masses of the those two cases lie above and below the $K\bar{K}$ threshold respectively.
- The widths of the $f_0(980)$ are rather similar in both cases.
- Both of these two poles are found in the RS II.

[1] R. Garcia-Martin, R. Kaminski, J. R. Pelaez, and J. Ruiz de Elvira, Phys. Rev. Lett. 107, 072001 (2011), 1107.1635.

[2]R. Garcia-Martin, R. Kaminski, J. R. Pelaez, J. Ruiz de Elvira, and F. J. Yndurain, Phys. Rev. D 83, 074004 (2011).

[3] Z.-H. Guo, J. A. Oller, and J. Ruiz de Elvira, Phys. Rev. D 86, 054006 (2012)

Corresponding to GKPY pole

X	RS	$\lvert\gamma_{\pi\pi}\rvert$ (GeV)	$\lvert\gamma_{K\bar{K}}\rvert$ (GeV)	Γ_1 (MeV)	Γ_2 (MeV)	$X_{\pi\pi}$	$X_{K\bar{K}}$
1.0	II	2.37 ± 0.21	5.21 ± 0.26	108.3 ± 18.9	54.3 ± 10.6	0.042 ± 0.007	0.958 ± 0.007
0.8	II	2.24 ± 0.20	4.65 ± 0.23	97.2 ± 16.9	43.2 ± 8.4	0.038 ± 0.007	0.762 ± 0.007
0.6	II	2.11 ± 0.19	4.01 ± 0.19	86.1 ± 14.8	32.1 ± 6.2	0.033 ± 0.006	0.567 ± 0.006
0.4	II	1.97 ± 0.17	3.24 ± 0.15	75.0 ± 12.9	21.0 ± 4.0	0.029 ± 0.005	0.371 ± 0.005
0.2	II	1.82 ± 0.16	2.23 ± 0.09	63.9 ± 11.0	9.9 ± 1.8	0.025 ± 0.004	0.175 ± 0.004

No solution for X=0.

r_{exp}	RS	$\lvert\gamma_{\pi\pi}\rvert$(GeV)	$\lvert\gamma_{K\bar{K}}\rvert$(GeV)	Γ_1(MeV)	Γ_2(MeV)	$X_{\pi\pi}$	$X_{K\bar{K}}$
0.52 [1]	II	2.03 ± 0.18	3.62 ± 0.32	79.9 ± 14.5	25.9 ± 4.7	0.031 ± 0.006	0.46 ± 0.20
0.68 [2]	II	1.92 ± 0.17	2.95 ± 0.26	71.3 ± 13.0	17.3 ± 3.1	0.028 ± 0.005	0.31 ± 0.13
0.75 [3]	II	1.87 ± 0.17	2.61 ± 0.23	67.5 ± 12.3	13.5 ± 2.5	0.026 ± 0.005	0.24 ± 0.11

[1] B. Aubert et al. (BaBar), Phys. Rev. D 74, 032003 (2006).

[2] J. A. Oller and E. Oset, Nucl. Phys. A 620, 438 (1997).

[3] W. Wetzel et al. Nucl. Phys. B 115, 208 (1976).

- Input pole parameter of $a_0(980)$:

Coupled-channel analysis of antiproton-proton annihilation data [1].
In Sheet II,

$$m_R = 1004.1 \pm 6.67 \text{ MeV}, \Gamma_R = 97.2 \pm 6.01 \text{ MeV}, \Gamma_{K\overline{K}}/\Gamma_{\pi\eta} = (13.8 \pm 3.5)\ \%$$

and in the Sheet III,

$$m_R = 1002.4 \pm 6.55 \text{ MeV}, \Gamma_R = 127.0 \pm 7.08 \text{ MeV}, \Gamma_{K\overline{K}}/\Gamma_{\pi\eta} = (14.9 \pm 3.9)\ \%$$

r_{exp}	RS	$\lvert\gamma_{\pi\eta}\rvert$(GeV)	$\lvert\gamma_{K\bar{K}}\rvert$(GeV)	Γ_1(MeV)	Γ_2(MeV)	$X_{\pi\eta}$	$X_{K\bar{K}}$
0.85[2]	II	2.90 ± 0.05	2.32 ± 0.08	111.8 ± 4.2	14.6 ± 0.6	0.100 ± 0.004	0.132 ± 0.009
	III	2.86 ± 0.05	2.61 ± 0.72	108.0 ± 3.7	19.1 ± 0.7	0.098 ± 0.004	0.249 ± 0.018
0.87[3]	II	2.88 ± 0.05	2.16 ± 0.07	109.8 ± 4.2	12.6 ± 0.5	0.098 ± 0.004	0.115 ± 0.008
	III	2.89 ± 0.05	2.43 ± 0.07	110.5 ± 3.8	16.5 ± 0.6	0.100 ± 0.004	0.216 ± 0.015

[1] M. Albrecht et al. (Crystal Barrel), Eur. Phys. J. C 80, 453 (2020), 1909.07091.

[2] P. A. Zyla et al. (Particle Data Group), PTEP 2020, 083C01 (2020).

[3] A. Abele et al., Phys. Rev. D 57, 3860 (1998).

- As increase of the branching decay ratio to the lighter channel, r_{exp}, the total compositeness X decrease.
- This is due to the increase of the coupling for the heavier $K\bar{K}$ channel with increasing X.

Figure: The total compositeness X as a function of the input branching ratio ($r_{\rm exp}$) when applying the method S. Panel (a) corresponds to the $f_0(980)$,Panel (b) corresponds to the $a_0(980)$.

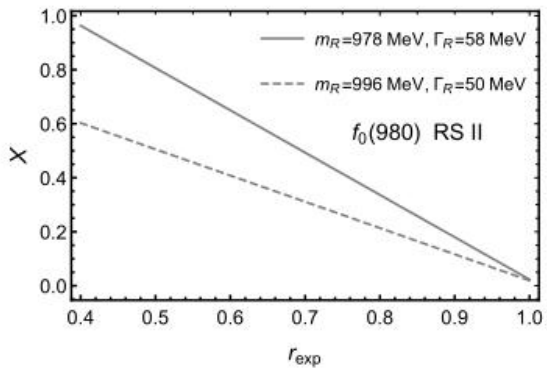

(a)

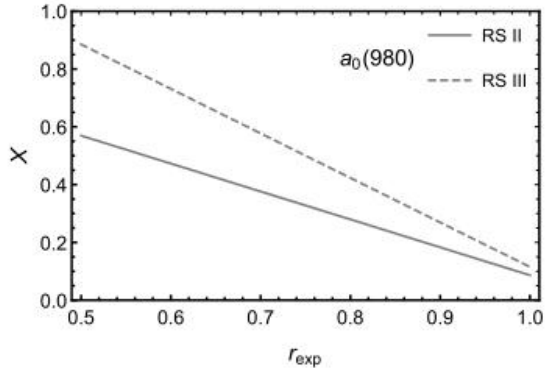

(b)

Flatté Parameterization

- The disadvantage of the approach followed above is the necessity to assume a value of n in $m_R + n\Gamma_R$ for the upper limit of integration.
- Since the $f_0(980)$ and $a_0(980)$ lie very close to the $K\bar{K}$ threshold, Flatté parameterization is very suitable to study those cases.
- This study stresses the need to distinguish between the bare and dressed couplings and widths in a Flatté parameterization.
- We reinterpret the relation between the total decay width and the partial width when the pole lies in the second Riemann Sheet.

- We consider the propagator of a resonance following the Flatté parameterization [1]

$$D(E) = E - E_f + \frac{i}{2}\widetilde{\Gamma}_1 + \frac{i}{2}g_2\sqrt{m_K E}\ .$$

We look for the zero of $D(E_R) = 0$ to determine the resonance pole positic $E_R = M_R - i\Gamma_R/2$.

- g_i is the bare coupling squared for the i_{th} channel
- The bare width $\widetilde{\Gamma}_1$ can be expressed as

$$\widetilde{\Gamma}_1 = \frac{q_1(m_R)g_1}{8\pi m_R^2}$$

- The Flatté parameterization contains as free parameters E_f, $\widetilde{\Gamma}_1$ and g_2

$\longrightarrow$ We need three equation to fix E_f, $\widetilde{\Gamma}_1$ and g_2.

[1] V. Baru, J. Haidenbauer, C. Hanhart, Y. Kalashnikova, and A.E. Kudryavtsev, Evidence that the a(0)(980) and f(0)(980) are not elementary particles, Phys. Lett. B 586, 53 (2004).

- Two main equations: the mass and width equation

$$M_R = \frac{\Gamma_R^2}{4\widetilde{\Gamma}_1} \cot\frac{\phi}{2}\left[1-\left(\frac{\widetilde{\Gamma}_1}{\Gamma_R}\tan\frac{\phi}{2}\right)^2\right],$$

$$\Gamma_R = \widetilde{\Gamma}_1 - \frac{\sigma}{2}\sqrt{m_K g_2^2 \widetilde{\Gamma}_1 |\tan\frac{\phi}{2}|}\,.$$

- where $\phi = \arctan\frac{\widetilde{\Gamma}_1/2}{E_f - m_K g_2^2/16}$ and M_R is the mass respect to $2m_K$.
- $\sigma = \pm 1$ comes from square root in solving equations.
- For formulas $\sqrt{E_R} = \frac{2i}{g_2\sqrt{m_K}}(M_R - E_f) + \frac{\Gamma_R - \widetilde{\Gamma}_1}{g_2\sqrt{m_K}}$ one can verify $\sigma = -1 \Leftrightarrow M_R - E_f < 0 \Leftrightarrow$ RS III, and $\sigma = +1 \Leftrightarrow M_R - E_f > 0 \Leftrightarrow$ RS II

From Baru, Haidenbauer, Hanhart et al., PLB 586 (2004) 53-61

Table 2
Parameters and results for the f_0 meson. The values M_R, $\Gamma_{\pi\pi}$ and E_f are given in MeV, r_e and a in fm, and k_1 and k_2 in MeV/c.

Ref.	M_R	$\Gamma_{\pi\pi}$	$\bar{g}_{K\bar{K}}$	E_f	r_e	a	k_1	k_2	W_{f_0}
[22]	969.8	196	2.51	-151.5	-0.63	1.15-i0.74	-58+i107	58-i729	0.17
[23]	975	149	1.51	-84.3	-1.05	0.99-i0.88	-65+i97	65-i477	0.23
[21]	973	253	2.84	-154	-0.56	1.09-i0.89	-69+i100	69-i804	0.14
[24]	996	128.8	1.31	+4.6	-1.22	-0.14-i 1.99	-84+i17	84-i351	0.21

The value of $\Gamma_{\pi\pi}$ ***are much larger than*** pole width of $f_0(980)$, and the same also holds form $a_0(980)$.

H. Y. Cheng, C. W. Chiang, and Z. Q. Zhang,
PRD 105 (2022) 3, 033006

a footnote

[5] From the amplitude analysis of the $\chi_{c1} \to \eta\pi^+\pi^-$ decay, BESIII obtained another set of couplings: $g_{a_0\to\eta\pi} = (4.14 \pm 0.02)\,\text{GeV}$ and $g_{a_0\to K\bar{K}} = (3.91 \pm 0.02)\,\text{GeV}$ [72]. However, this set of couplings is not appealing for two reasons: (a) the large coupling constant $g_{a_0\to\eta\pi}$ will yield too large partial width $\Gamma_{\eta\pi} = 222$ MeV, recalling that the total width of $a_0(980)$ lies in the range of 50 to 100 MeV [1], and (b) it is commonly believed that $a_0(980)$ couples more strongly to $K\overline{K}$ than to $\eta\pi$, especially in the scenario in which $a_0(980)$ is a $K\overline{K}$ molecular state.

- Let us denote by β the residue of $1/D(E)$ at the resonance pole,

$$\beta = \left| \lim_{E \to E_R} \frac{E - E_R}{D(E)} \right| = \left| \frac{1}{1 + \frac{ig_2}{4}\sqrt{\frac{m_K}{E_R}}} \right| = \frac{\sqrt{8u}}{\left(g_2^2 m_K + 8u + 4\sigma g_2 \sqrt{m_K (u - 2M_R)} \right)^{1/}}$$

- The relation between *dressed* coupling squared $|\gamma_i^2|$ and the bare one g_i

$$\begin{aligned} |\gamma_1|^2 &= g_1 \beta \,, \\ |\gamma_2|^2 &= 32\pi m_K^2 g_2 \beta \,, \end{aligned}$$

- The decay width relation

$$\begin{aligned} D(E) &= E - E_f + \frac{i}{2}\left[\widetilde{\Gamma}_1 + 2g_2 \sqrt[II]{m_K E}\right] - \frac{i}{2} g_2 \sqrt[II]{m_K E} \\ &= E - E_f + \frac{i}{2}\left[\widetilde{\Gamma}_1 - 2g_2 \sqrt[III]{m_K E}\right] + \frac{i}{2} g_2 \sqrt[III]{m_K E} \,. \end{aligned}$$

- In the RS II, the momentum p_2 changes sign with respect to RS III while p_1 does not: $\sqrt[III]{E} = -\sqrt[II]{E}$

- Again scenarios of taking either X or $r_{\rm rexp}$ as input
- Recalling the aforementioned equations $X = X_1 + X_2$, we have for X_1 and X_2,

$$\begin{aligned} X_1 &= |\gamma_1|^2 \left|\frac{\partial G_1}{\partial s}\right|_{s=s_R} = \frac{8\pi m_R^2 \widetilde{\Gamma}_1}{p_1(m_R)} \beta \left|\frac{\partial G_1}{\partial s}\right|_{s=s_R}, \\ X_2 &= 32\pi m_K^2 g_2 \beta \left|\frac{\partial G_1}{\partial s}\right|_{s=s_R} \end{aligned}$$

- For r_{exp} as input, we have following formulas

$$r_{\rm exp} = r\beta = \frac{\sqrt{2u}\left(2\sqrt{u-2M_R} + g_2\sigma\sqrt{m_K}\right)}{\sqrt{u-2M_R}\left(g_2^2 m_K + 8u + 4\sigma g_2\sqrt{m_K(u-2M_R)}\right)^{1/2}}, \text{RS III}$$

$$2 - r_{\rm exp} = r\beta = \frac{\sqrt{2u}\left(2\sqrt{u-2M_R} + g_2\sigma\sqrt{m_K}\right)}{\sqrt{u-2M_R}\left(g_2^2 m_K + 8u + 4\sigma g_2\sqrt{m_K(u-2M_R)}\right)^{1/2}}, \text{RS II}$$

Table: Method F applied to the resonance $f_0(980)$ with pole position in the RS II (column 2) from Eq. (1): The value of X taken as input is given in the first column. We calculate the bare width $\widetilde{\Gamma}_1$ (column 3), the bare coupling g_2 (column 4), E_f (column 5), Γ_1 (column 6), Γ_2 (column 7), X_1 (column 8), and X_2 (column 9).

X	RS	$\widetilde{\Gamma}_{\pi\pi}$(MeV)	g_2	E_f(MeV)	Γ_1(MeV)	Γ_2(MeV)	$X_{\pi\pi}$	$X_{K\bar{K}}$
0.8	II	948.3 ± 383.1	10.01 ± 4.03	-389.7 ± 210.7	84.4 ± 15.3	30.4 ± 8.3	0.033 ± 0.006	0.767 ± 0.006
0.6	II	200.3 ± 38.5	1.63 ± 0.23	-57.6 ± 19.3	80.4 ± 14.4	26.4 ± 7.0	0.031 ± 0.006	0.569 ± 0.006
0.4	II	113.2 ± 20.1	0.66 ± 0.07	-20.4 ± 8.6	73.2 ± 12.9	19.2 ± 4.9	0.028 ± 0.005	0.372 ± 0.005
0.2	II	75.2 ± 13.0	0.24 ± 0.02	-4.2 ± 5.3	63.9 ± 11.1	9.9 ± 2.4	0.025 ± 0.004	0.175 ± 0.004

Table: Method F applied to the resonance $f_0(980)$ with the pole position in the RS II from Eq. (1): The branching ratio r_{exp} is taken as input.

r_{exp}	$\widetilde{\Gamma}_{\pi\pi}$ (MeV)	g_2	E_f (MeV)	Γ_1 (MeV)	Γ_2 (MeV)	$X_{\pi\pi}$	$X_{K\bar{K}}$
0.52	$(71, 2623)$	$(0.36, 26.8)$	$(-21.2, 1167.2)$	79.9 ± 14.5	25.9 ± 4.7	0.030 ± 0.006	0.48 ± 0.22
0.68	113.8 ± 38.3	0.69 ± 0.45	$(-66.7, 6.3)$	71.3 ± 13.0	17.3 ± 3.1	0.028 ± 0.005	0.35 ± 0.18
0.75	89.4 ± 20.4	0.41 ± 0.17	$(-42.9, 7.7)$	67.5 ± 12.3	13.5 ± 2.5	0.026 ± 0.005	0.26 ± 0.14

The spectral density function

- The approach is based on integrating the spectral density of a bare elementary discrete state around the resonance signal region, The W_R is calculated as [1]

$$W_R = \int_{-\Delta}^{+\Delta} dE\, \omega(E)\,,$$

$$\omega(E) = \frac{1}{2\pi} \frac{\widetilde{\Gamma}_1 + g_2\sqrt{m_K E}\theta(E)}{\left(E - E_f - \frac{1}{2}g_2\sqrt{-m_K E}\theta(-E)\right)^2 + \frac{1}{4}\left(\widetilde{\Gamma}_1 + g_2\sqrt{m_K E}\theta(E)\right)^2}\,,$$

- The value of W_R is the probability for finding the bare state dependent on integral interval Δ.
- The compositeness X can be calculated as $1 - W_R$.

[1] V. Baru, J. Haidenbauer, C. Hanhart, Y. Kalashnikova, and A. E. Kudryavtsev, Phys. Lett. B 586, 53 (2004), arXiv:hep-ph/0308129.

Figure: The spectral density function $\omega(E)$ is shown for the $f_0(980)$ in the left upper panel and for the $a_0(980)$ in the right lower one.

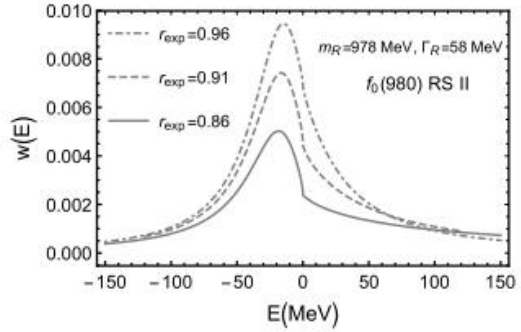

(a)

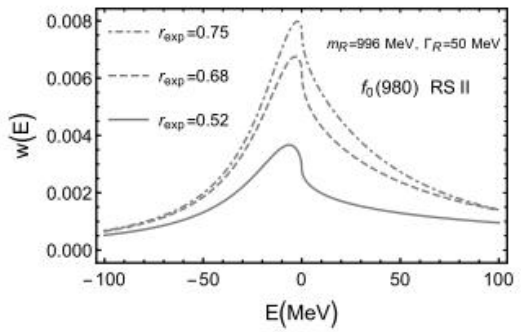

(b)

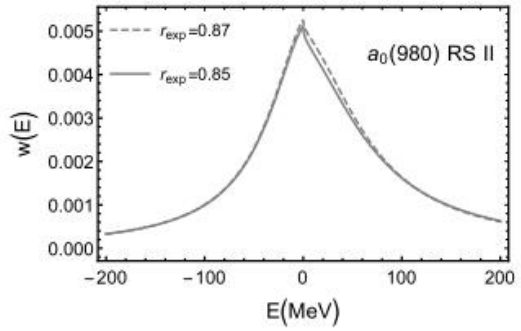

(c)

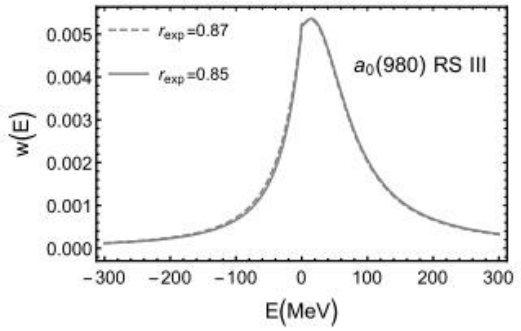

(d)

Table: Resonance $f_0(980)$ with the pole position in the RS II from Eq. (1): We show the dependence of W_{f_0} on the integration interval $[-\Delta, \Delta]$ with Δ up to $2\Gamma_R$. For the experimental inputs of $r_{\rm exp}$ we give our final estimate for $1 - W_{f_0}$ in the column 5. The total compositeness $X = X_1 + X_2$ from Method F is given in the last column.

$r_{\rm exp}$	$[-\Delta, \Delta]$	W_{f_0}	$(1 - W_{f_0})_\Delta$	$1 - W_{f_0}$	X
0.52	$[-25, 25]$	0.13	0.87		
	$[-50, 50]$	0.21	0.79		
	$[-75, 75]$	0.27	0.73		
	$[-100, 100]$	0.31	0.69	0.76 ± 0.15	0.51 ± 0.22
0.68	$[-25, 25]$	0.25	0.75		
	$[-50, 50]$	0.39	0.61		
	$[-75, 75]$	0.47	0.53		
	$[-100, 100]$	0.53	0.47	0.57 ± 0.15	0.38 ± 0.18
0.75	$[-25, 25]$	0.30	0.70		
	$[-50, 50]$	0.45	0.55		
	$[-75, 75]$	0.55	0.45		
	$[-100, 100]$	0.61	0.39	0.50 ± 0.15	0.29 ± 0.14

Table: Resonance $a_0(980)$ with the pole position in the RS II from Eq. (1). The dependence of W_{a_0} on the integration interval $[-\Delta, \Delta]$ for the $a_0(980)$ is shown with Δ up to $2\Gamma_{a_0}$. In the column 5 we provide our interval estimated for $1 - W_{a_0}$ and in the last one $X = X_1 + X_2$ from is given.

$r_{\rm exp}$	$[-\Delta, \Delta]$	W_{a_0}	$(1 - W_{a_0})_\Delta$	$1 - W_{a_0}$	X
0.85	$[-50, 50]$	0.38	0.62		
	$[-100, 100]$	0.57	0.43		
	$[-150, 150]$	0.67	0.33		
	$[-200, 200]$	0.73	0.27	$0.33 - 0.43$	0.216 ± 0.017
0.87	$[-50, 50]$	0.39	0.61		
	$[-100, 100]$	0.59	0.41		
	$[-150, 150]$	0.68	0.32		
	$[-200, 200]$	0.74	0.26	$0.32 - 0.41$	0.198 ± 0.016

Is it tea or coffee?

a hard question